Supporting Information

Zhao et al. 10.1073/pnas.1204460109

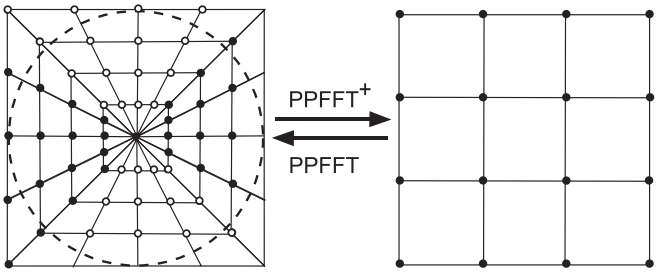

Fig. S1. Geometrical relationship between a pseudopolar and a Cartesian grid. For an N x N Cartesian grid, the corresponding pseudopolar grid is defined by a set of $2N$ lines, each line consisting of $2N$ grid points mapped out on N concentric squares with $n = 4$ in this example (*Left*). The $2N$ lines are subdivided into a basically horizontal (BH) group defined by $y = sx$, where $|s| \leq 1$, and a basically vertical (BV) group defined by $x = sy$, where $|s| \leq 1$; the BH and BV groups are symmetric under the interchange of x and y, and $\Delta s = 2/N$. The circle with dashed line on the pseudopolar grid represents the resolution circle and the grid points outside the circle cannot be obtained from the Fourier transform of the measured projections.

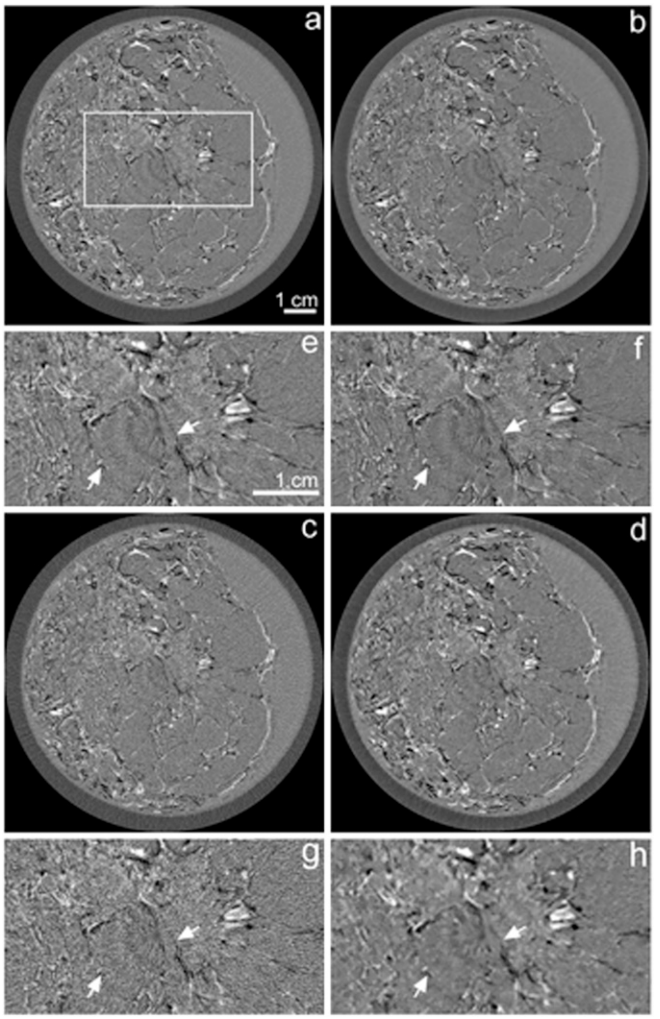

Fig. S2. A 92-μm-thick axial slice reconstructed by FBP 2000 (*A*), EST 512 (*B*), FBP 512 (*C*), and EST 200 (*D*), in which the white rectangle indicates a tumor region. Zoomed view of the tumor region (the white rectangle) reconstructed by FBP 2000 (*E*), EST 512 (*F*), FBP 512 (*G*), and EST 200 (*H*), in which the white arrows indicate the visibility of detailed features inside the tumor regions. A Hamming filter was used in the FBP reconstructions, whereas a nonlocal means filter was applied to the EST reconstructions.

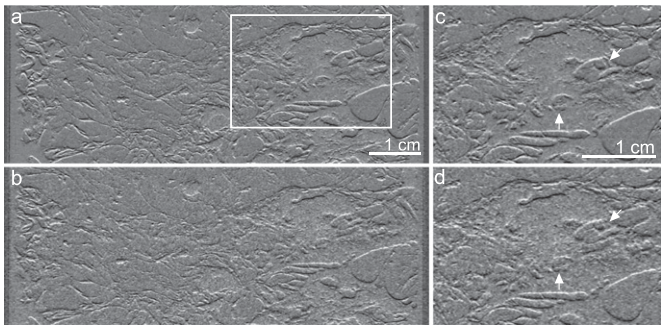

Fig. S3. Image quality comparison between EST 512 (*A*) and FBP 512 (*B*). A nonlocal means filter was applied to both the EST and FBP reconstructions. (*C* and *D*) Zoomed view of the tumor region by EST 512 (*C*) and FBP 512 (*D*). The white arrows indicate that, with the same nonlocal means filter, EST 512 shows more fine features in the tumor region than FBP 512.

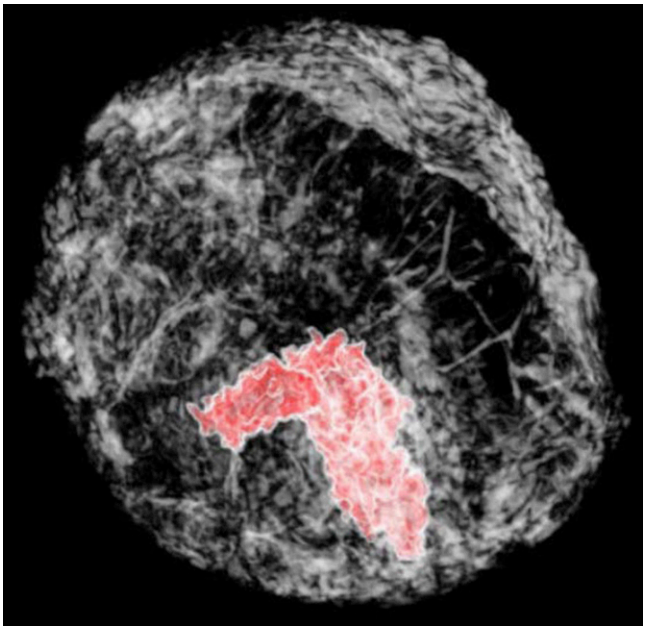

Movie S1. Three-dimensional volume renderings of the EST 512 reconstruction, in which the 3D segmented tumor (in red) and its surrounding tissues such as skin, lobules, and lactiferous duct are clearly visible.

Movie S1